ISSN 1995-0780, Nanotechnologies in Russia, 2015, Vol. 10, Nos. 5–6, pp. 370–379. © Pleiades Publishing, Ltd., 2015.
Original Russian Text © E.A. Eremina, E.E. Ondar, A.V. Sidorov, A.V. Grigor'eva, E.A. Gudilin, 2015, published in Rossiiskie Nanotekhnologii, 2015, Vol. 10, Nos. 5–6.

Reduced Graphite Oxide Decorated with Gold Nanoparticles for Raman Scattering Spectroscopy

E. A. Eremina[a], E. E. Ondar[a], A. V. Sidorov[b], A. V. Grigor'eva[b], and E. A. Gudilin[a,b]

[a] *Faculty of Chemistry, Moscow State University, Moscow, 119992 Russia*

[b] *Faculty of Material Sciences, Moscow State University, Moscow, 119992 Russia*

e-mail: ea_er@mail.ru

Received November 25, 2014; accepted for publication February 12, 2015

Abstract—Surface-enhanced Raman scattering (RS) spectroscopy is a sensitive analytical method that makes it possible to detect individual molecules. The substantial enhancement of the intensity of the signals in this method when compared to traditional Raman scattering is associated with two mechanisms, namely, electromagnetic and chemical. The first mechanism is associated with the enhancement of both the impinging and scattered radiation (electromagnetic enhancement), while the second mechanism is explained by the electron interaction between the molecule being analyzed and metal nanoparticles, namely, by the change in the polarizability of the adsorbed molecule, which results in the displacement and broadening of the electron levels of the adsorbed molecule or in the occurrence of new levels and promotes the enhancement of the signal in the Raman scattering spectrum. Graphene and material associated with it such as graphene oxide, graphite oxide, and reduced forms of graphene and graphite oxides are advanced materials for the creation of a significant chemical enhancement. Taking into account the different nature of the enhancement of the signal from the nanoparticles of noble metals and graphene and its derivatives, it is reasonable to study the effectiveness of hybrid structures on the basis of derivatives of graphene and noble metal nanoparticles in the Raman scattering spectroscopy of the analyte molecules with an aromatic structure.

DOI: 10.1134/S1995078015030052

INTRODUCTION

Surface-enhanced Raman scattering (RS) spectroscopy or hyper-Raman scattering (HRS) spectroscopy is a sensitive analytical method that makes it possible to detect individual molecules. A substantial enhancement of the intensity of the signals in this method when compared to the traditional method of RS is associated with two mechanisms, namely, electromagnetic and chemical. The first mechanism is due to the enhancement of both the impinging and scattered radiation (electromagnetic enhancement), while the second mechanism is explained by the electron interaction between the molecule being analyzed and metal, namely, by the change in polarizability of the adsorbed molecule, which results in the displacement and broadening of the electron levels of the adsorbed molecule or in the occurrence of new levels and promotes the enhancement of the signal in the Raman scattering spectrum [1].

Graphene and material associated with it such as graphene oxide, graphite oxide (GO), and reduced forms of graphene and graphite oxides are the advanced materials for the creation of a significant chemical enhancement [2]. Graphene possesses a high mobility of electrons (200000 $cm^2 V^{-1} s^{-1}$); electrical conductivity; and acceptable mechanical, chemical, and optical characteristics. This makes it possible to consider graphene a prospective candidate for the creation of hybrid structures with gold nanoparticles for the enhancement of the signal from the analyte molecules in the RS spectrum. GO that is a precursor of chemically synthesized graphene can also act as a carrier of nanoparticles of noble metals. In addition to the developed surface, the interest in GO is determined by the presence of oxygen-containing functional groups formed during the oxidation of graphite, which promotes the additional retention of the noble metal nanoparticles on the surface of GO due to chemisorption, which makes it possible to improve the accuracy of the analyses. The material is an insulator and the specific surface area of GO can reach 2600 m^2/g according to literature data [3].

Reduced graphite oxide (RGO), for which the recovery of the continuous system of π bonds violated in GO is characteristic, is another promising material for the creation of HRS-active composites with noble-metal nanoparticles. As opposed to GO, this material has conductivity of about 1 kOhm/cm^2 [4]. Materials on the basis of graphene are atomically flat, which is why the effective charge transfer between the carbon-containing layer and analyte molecule is possible in them. Chemical enhancement occurs due to the

interaction and charge transfer from the oxygen-containing functional groups of the derivatives of graphene. The largest enhancement is observed for defective graphene, in which there are functional groups prone to the charge transfer. The oxidation and *p*-type doping of graphene results in the chemical enhancement of the signal for the analyte molecules possessing aromatic structure by 10^4 times when compared to ideal graphene. Partially reduced graphene oxide demonstrates the enhancement of the signal by 10^3 times.

Taking into account the different nature of the enhancement of the signal from noble-metal nanoparticles and graphene and its derivatives, it is reasonable to study the effectiveness of hybrid structures on the basis of derivatives of graphene and noble-metal nanoparticles in the RS spectroscopy of analyte molecules with an aromatic structure.

EXPERIMENTAL

Reagents. Graphite (TIMCAL TIMREX® KS4), $HAuCl_4$ (0.05 M), $AgNO_3$ (Carl Roth, analytical reagent (AR) grade), NaOH (AR grade), $KMnO_4$ (AR grade), $NaNO_3$ (chemically pure), H_2SO_4 (conc.), H_2O_2 (3%), $(NH_2)_2CS$ (AR grade), $(NH_2)_2CO$ (AR grade), glycine $C_2H_5O_2N$ (AR grade), L-cysteine $C_3H_7NO_2S$ (AR grade), sodium citrate $Na_3C_6H_5O_7$ (34 mM), NH_3 (conc.), H_2O (dist.), and C_2H_5OH (Ferein, 95%) were used as the initial reagents.

Preparation of GO. GO was obtained according to the Hummers method [5]. Four grams of graphite, 2 g of sodium nitrate, and 83.1 mL of 98% sulfuric acid was placed into a two-neck reaction flask cooled in an ice bath. Potassium permanganate (12 g in total) was added to the obtained reaction mixture every ten minutes, keeping the temperature of the solution below 20°C, after which the ice bath was replaced by a bath with warm water ($T \sim 36$°C); here, the temperature of the solution increased from 17°C to 35°C. Then 184 mL of distilled water was gradually added over 30 min, keeping the temperature of the solution below 70°C. During the addition of water, the change in the coloration from black-gray to brown was observed.

The solution was stirred for 15 min, and then 560 mL of distilled water and 212 mL of a 3% hydrogen peroxide solution was added, which resulted in the occurrence of dark green coloration.

In 12 h, the yellow-brown solution was decanted and then centrifuged at 9 000 rpm for 10 min at room temperature. The precipitates were dissolved in distilled water several times and subjected to repeated decanting until the pH of the aqueous solution of GO reached 7. The estimate concentration of the obtained solution of GO was 1.11 M.

Preparation of RGO. L-cysteine, glycine, urea, and thiourea in an amount that twice exceeded the amount of GO was chosen as the reducing agents for GO. The solutions of the reducing agents were added to the 0.625 M solutions of GO with a volume of 13 mL each. Dry reducing agents (1.235 g of $(NH_2)_2CS$, 0.975 g of $(NH_2)_2CO$, and 1.22 g of NH_2CH_2COOH) were dissolved in 10 mL of water each and added to the solution of GO. L-cysteine (1.96 g) was added to the solution of GO without any additional dissolution in water. The mixtures were stirred on magnetic stirrers at room temperature for 15 h.

The obtained samples were centrifuged (9000 rpm, 10 min) at room temperature and rinsed with distilled water and ethanol to a neutral pH value of the solution. The products were dried in a dessicator over P_2O_5.

Preparation of the gold nanoparticles. The synthesis of the gold nanoparticles was carried out according to the Turkevich method [6]. Fifty milliliters of water was added to 300 μL of 0.05 M solution of $HAuCl_4$ and brought to boil upon continuous stirring. Three milliliters of the solution of sodium citrate was added to the solution and the stirring was continued for 3 min; here, the change in the coloration of the solution from pale violet to intensive ruby red was observed, after which the heating was continued for additional 10 min. The solution was cooled down to room temperature upon continuous stirring on a magnetic stirrer.

Preparation of the GO–gold nanoparticles composites. The graphene oxide–gold nanoparticle composite was synthesized by preparing the gold nanoparticles according to the Turkevich method in the presence of GO. Five hundred microliters of 34 mM solution of sodium citrate was added to the boiling solution obtained from 150 mL of distilled water, 730 μL of the 0.05 M solution of $HAuCl_4$, and 2 mL of the 0.625 M suspension of graphene oxide upon intensive stirring. After being kept at the boiling point for 15 min, the change in the coloration of the solution from grey to violet and wine red was observed.

The samples were centrifuged (6000 rpm, 5 min), decanted, and rinsed with distilled water. The suspension was stored in a closed container in a dark place.

Preparation of the RGO–gold composites. The weights of the reducing agents being added were calculated in such a way that the amount of the reducing agent was twice that of the amount of graphene oxide in terms of the molar ratio. Three hundred microliters of the 0.05 M solution of $HAuCl_4$ and 50 mL of water was placed into beakers preliminarily rinsed with *aqua regia* and the mixture was brought to a boil while stirred on a magnetic stirrer. After the onset of boiling, 150 μL of 1.11 M GO and 0.036 g of crystalline L-cysteine was added to the first beaker (sample 1) and the heating was ceased, after which the solution turned brown. Into the five remaining beakers, 3 μL of 34 mM sodium citrate was added and the development of the ruby red coloration of the solutions 2–6 gave evidence of the formation of gold nanoparticles. After this, 150 μL of GO was added to samples 2–6 and different reducing agents were added to samples 3–6 as follows:

Table 1. Information on the samples of GO, RGOs, and composites

Number of the sample	Reducing agent for GO	Scheme of the performed reaction	Abbreviation used in the work
1	L-cysteine	$HAuCl_4$ + GO + L – cys_{solid}	$HAuCl_4$ + GO + cysteine
2	GO without the reducing agent (control sample)	(*), AuNP + GO	AuNP + GO
3	L-cysteine	(*), AuNP + GO + L – cys_{solid}	AuNP + GO + cysteine RGO_CYS
4	Glycine	(*), AuNP + GO + gly_{solid}	AuNP + GO + glycine RGO_GLY
5	Thiourea	(*), AuNP + GO + $(NH_2)_2CS_{solid}$	AuNP + GO + thiourea RGO_$(NH_2)_2CS$
6	Urea	(*), AuNP + GO + $(NH_2)_2CO_{solid}$	AuNP + GO + urea RGO_$(NH_2)_2CO$

* Reaction of the formation of the gold nanoparticles: $HAuCl_4 + Na_3Cit \rightarrow AuNP$.

0.036 g of crystalline L-cysteine to sample 3, 0.025 g of crystalline glycine to sample 4, 0.028 g of thiourea to sample 5, and 0.018 g of urea to sample 6. All six solutions were left on the magnetic stirrer without heating for 24 h (Table 1).

Generalized information on all synthesized samples is presented in Table 1.

STUDY METHODS

The optical absorption spectra were registered on a PerkinElmer Lambda 950 UV/Vis/NIR scanning spectrophotometer (PerkinElmer, Unites States).

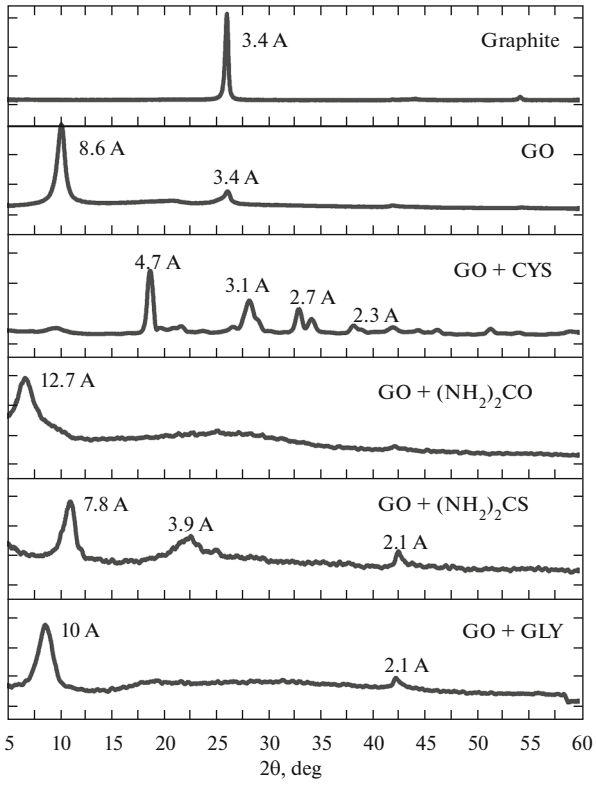

Fig. 1. Result of the XPA of the samples of initial graphite, GO, and RGO obtained under the action of the corresponding reducing agents.

An analysis of the electron diffraction and a detailed study of the microstructure was carried out using transmission electron microscopy (TEM) on a LEO 912 AB Omega microscope with a LaB_6 cathode with the accelerating potential of 100 kV (Carl Zeiss, Germany). During the registration of the electron diffraction, the length of the chamber was 265 mm and metal gold served as the standard.

The thermogravimetric analysis (TGA) and differential thermal analysis (DTA) was performed using a Netzsch STA 409 PC/PG thermoanalytical unit (Netzsch, Germany) in air in platinum crucibles within a temperature range of 40–800°C at a heating rate of 5°C/min (the weight of the sample was 20–40 mg).

The X-ray phase analysis (XPA) was carried out using a Rigaku D/MAX 2500 diffractometer (Rigaku, Japan) with the Bragg–Brentano geometry with a rotating anode (the CuK_α radiation). The registration was carried out in a step-by-step mode within the angle range $2\theta = 2°–80°$ in increments of 0.02° to 2θ at the exposition of 2 s per point. The data were processed using standard packages of the WinXpow software.

Studies by the method of RS spectroscopy and HRS spectroscopy were carried out using an InVia Reflex microscope (Renishaw, England) in a confocal mode with the use of a red laser (He/Ne, wavelength of 633 nm, 20 mW) and green laser (Ar, the wavelength of 514 nm, 20 mW). The capacity of the neutral density filter was 100% for the RS spectra and 10% for the HRS spectra. The time of signal acquisition was 10 s. The instrument was adjusted using monocrystalline silicon plates as the standard.

In order to obtain the RS spectra, 20 μL of the solution of the synthesized composite was applied on a glass support washed thoroughly in *aqua regia*. In order to obtain the HRS spectra, 10 μL of the solution of methylene blue with a concentration of 10^{-6} M was dropped onto the dried layer of the composite consisting of gold nanoparticles and material on the basis of GO. The supports were dried at room temperature in air, after which the spectral studies were conducted using a laser with a wavelength of 633 nm.

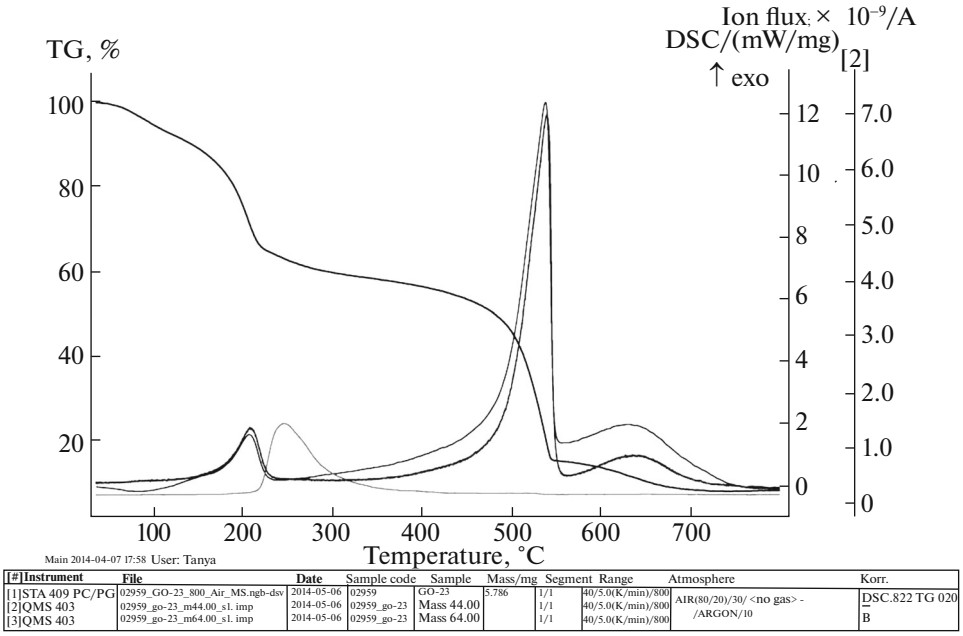

Fig. 2. Results of the thermogravimetric analysis of GO.

RESULTS AND DISCUSSION

X-ray phase analysis. The results of the XPA of initial graphite and composites on its basis are presented in Fig. 1. In the case of the initial sample of graphite, an intensive signal (002) at $2\theta = 26.2°$ is observed, which corresponds to the interplanar distance of 3.4 Å. A significant decrease in the intensity of the peak at $2\theta = 26.2°$ and the occurrence of the peak at $2\theta = 10.3°$ is observed in the X-ray diagram of the sample of GO, which gives evidence of the increase in the interplanar distance to 8.6 Å induced by the incorporation of the oxygen-containing groups and water molecules.

The X-ray diagrams of the samples of the reduced forms of GO differ from each other to a considerable extent. When cysteine, urea, and thiourea is used, the occurrence of the reflection corresponding to the interplanar distance of 3.1 Å is observed, which can be attributed to the formation of the reduced form RGO, for which the peak (002) observed for initial graphite is characteristic. The occurrence of the broadened reflections in the low-angle region in the case of the **RGO_$(NH_2)_2CO$**, **RGO_$(NH_2)_2CS$**, **RGO_GLY**, and **RGO_CYS** samples may give the evidence of the incorporation of amino groups present in the composition of the reducing agents into the interlaminar spaces of GO. Apparently, the formation of the hydrogen bonds between the C–OH–NH_2–R groups resulting in the protonation of amino groups (C–OH–NH_2–R → –COO–H_3N–R) is the basis for such an incorporation. The protonated amino groups bind to the surface of GO via the nucleophilic substitution of the epoxy groups, which is confirmed by the data of the thermal analysis of the samples under study.

Thermal analysis. It is seen from the data of the TG–DTA of GO presented in Fig. 2 that two types of transformations are observed during the heating of the sample from 40°C to 800°C. The first process accompanied by an insignificant *exo*-effect completes at around 200°C and the mass loss is around 30%. According to the data of the mass spectral analysis of the effluent gases, water and sulfur oxide SO_2 is the main products at this stage. The presence of the latter gas is apparently associated with the use of concentrated sulfuric acid during the synthesis of GO and is observed on the thermograms of all studied samples. The second stage of the transformation takes place within the temperature range of 450–550°C and is accompanied by a significant *exo*-effect, the release of carbon dioxide, and mass loss of up to 80% of the initial value. During the heating of the sample of GO to 800°C, the total mass loss is 91.2%. The curves of the DSC and temperature dependence of the release of carbon dioxide are almost identical because carbon is the main component of the sample under study.

Similar studies were conducted for all reduced forms of GO. The main regularities can be traced using the sample prepared by the reduction with glycine as the example. Three stages appear clearly on the TG and DSC curves of the RGO_GLY sample (Figs. 3a, 3b). According to the data of the mass spectral analysis, the release of N_2 and O_2 determined by the oxidation of the amino group present in the composition of glycine is the first process accompanied by the endothermic effect at around 80°C. At this stage, the mass losses are about 20 wt %. The intensive release of adsorbed water and carbon dioxide is observed within the temperature range around 200°C.

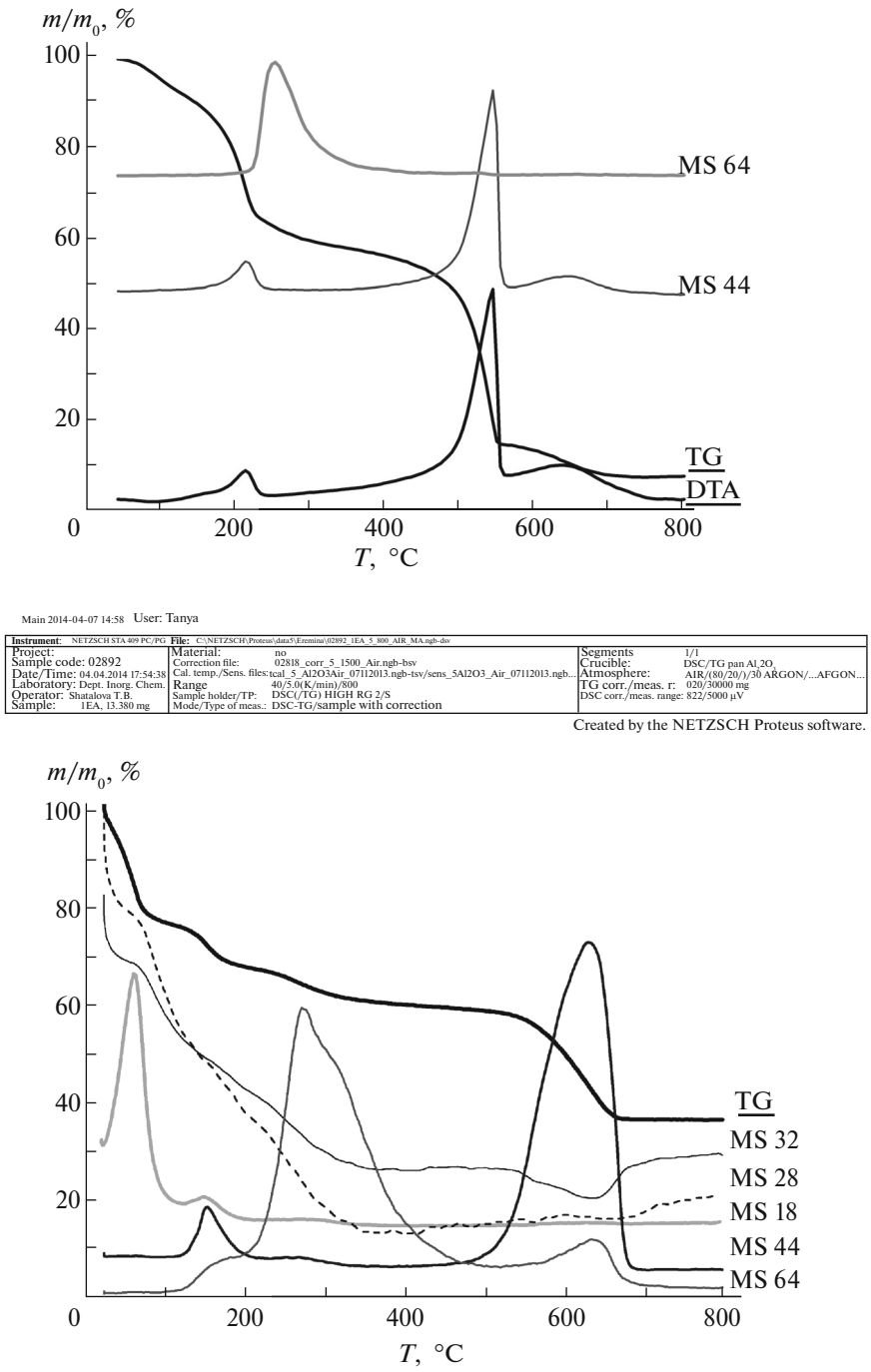

Fig. 3. Results of (a) thermogravimetric and (b) mass spectral analyses of GO reduced with glycine (RGO_GLY).

The total mass loss at this stage is 42 wt %. The third stage, within the temperature range of 500–600°C, is accompanied by the intensive exothermic effect and intensive release of CO_2. The total mass loss by the sample during heating to 700°C is about 75 wt %. The occurrence of the signal corresponding to the mass of 34 g, whose temperature dependence repeats the temperature dependence of oxygen, should be noted. This may give evidence of the formation of H_2O_2.

Analyzing the data of the thermal analysis of all synthesized samples, the following common features can be distinguished:

1. The process of the loss of water is generally two-stage and is completed at a temperature of about 200°C.

2. For all the samples, the presence of SO_2 determined by the chemical prehistory of the samples is characteristic.

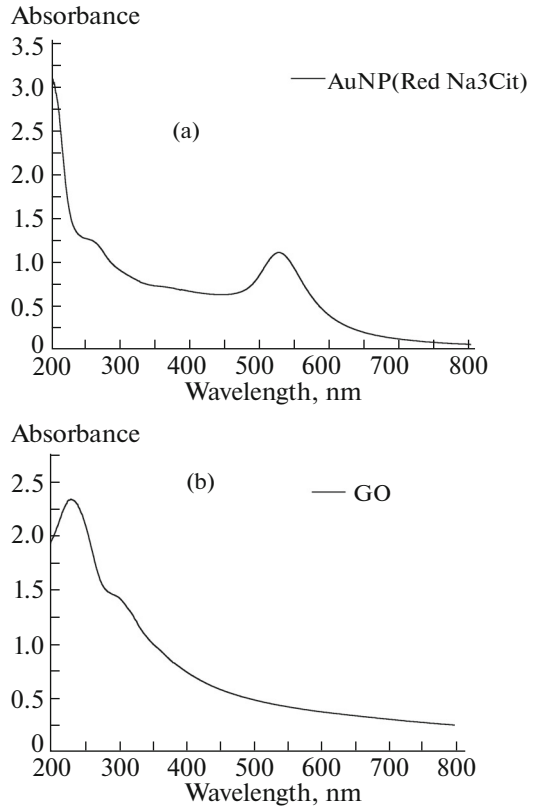

Fig. 4. Results of UV–visible spectroscopy of the solution of (a) gold nanoparticles and (b) GO.

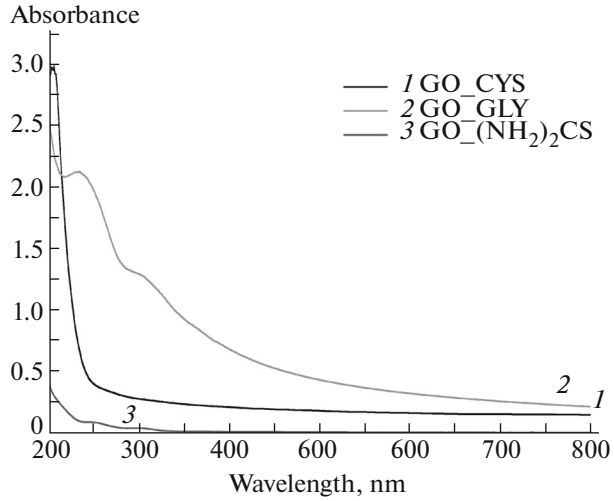

Fig. 5. Results of the UV–visible spectroscopy of the solutions of RGO.

3. For all the samples, the release of nitrogen that is the product of the oxidation of the reducing agent is characteristic.

4. Within the temperature range of 600–700°C, a significant exothermic effect determined by the combustion of the samples with the formation of CO_2 is observed.

UV–visible spectroscopy. It is apparent from the data of the UV–visible spectroscopy that the maximum of the absorption band of the gold nanoparticles is observed at $\lambda = 526$ nm, which is characteristic for gold colloids synthesized according to the Turkevich method (Fig. 4a). At the same time, a bend is observed near 260 nm in the UV spectrum, which gives evidence of the replacement of the ligands in the square chloride complex $[AuCl_4]^-$ and of the formation of the $[AuCl_3(OH)]^-$ complex [7]. In the UV spectrum of freshly prepared GO, an absorption maximum at $\lambda = 233$ nm, which is attributed to the C=C fragments in literature, and a shoulder at 300 nm, which is associated with the carbonyl groups, is observed (Fig. 4b). During the reduction of GO with cysteine and thiourea (Fig. 5), these bands disappear in the spectra, which gives evidence of the reduction of GO. When glycine is used as the reducing agent, the quantitative reduction of the chloride gold complex does not occur, which is seen by the absence of new absorption maximums in the visible region of the spectrum.

An analysis of the absorption spectrum of the solution obtained by the simultaneous pouring of three solutions—aurichlorohydric acid, sodium citrate, and suspension of GO—showed the presence of a maximum of the absorption band at around 520 nm, which gives evidence of the formation of gold nanoparticles (Fig. 6a). In addition, a shift in the absorption maximum of GO to 250 nm is observed. The shoulder at 300 nm becomes nearly invisible, which gives evidence of the reduction of GO. The presence of the absorption maximum at around 520 nm gives evidence of the possibility of enhancing the signal in the RS spectrum due to the resonance phenomena with a green laser (e.g., 514.5 nm).

In the spectra of the AuNP + RGO_$(NH_2)_2$CS and AuNP + RGO_$(NH_2)_2$CO samples (Figs. 6b, 6c), in which the suspension of GO and corresponding reducing agent was added to the formed solutions of the gold nanoparticles, the absorption band characteristic for the gold nanoparticles, the maximum of which is at $\lambda = 537$ nm and $\lambda = 520$ nm, respectively, appears clearly. As follows from the presented results, the shoulder at 300 nm, which is characteristic for the spectra of GO, is nearly invisible. These data give evidence of a reduction of GO with thiourea and urea, as well as of the formation of a composite consisting of gold nanoparticles and RGO.

An analysis of the optical spectra of the AuNP + RGO_CYS and AuNP + RGO_GLY samples (Fig. 6d) showed the absence of the absorption maximums in the visible region of the spectrum and, in particular, at 520 nm.

Transmission electron microscopy. The results of a study of the microstructure of the synthesized samples are presented in Fig. 7.

The corrugated lamellar structure of the obtained material appears clearly in the microphotographs of

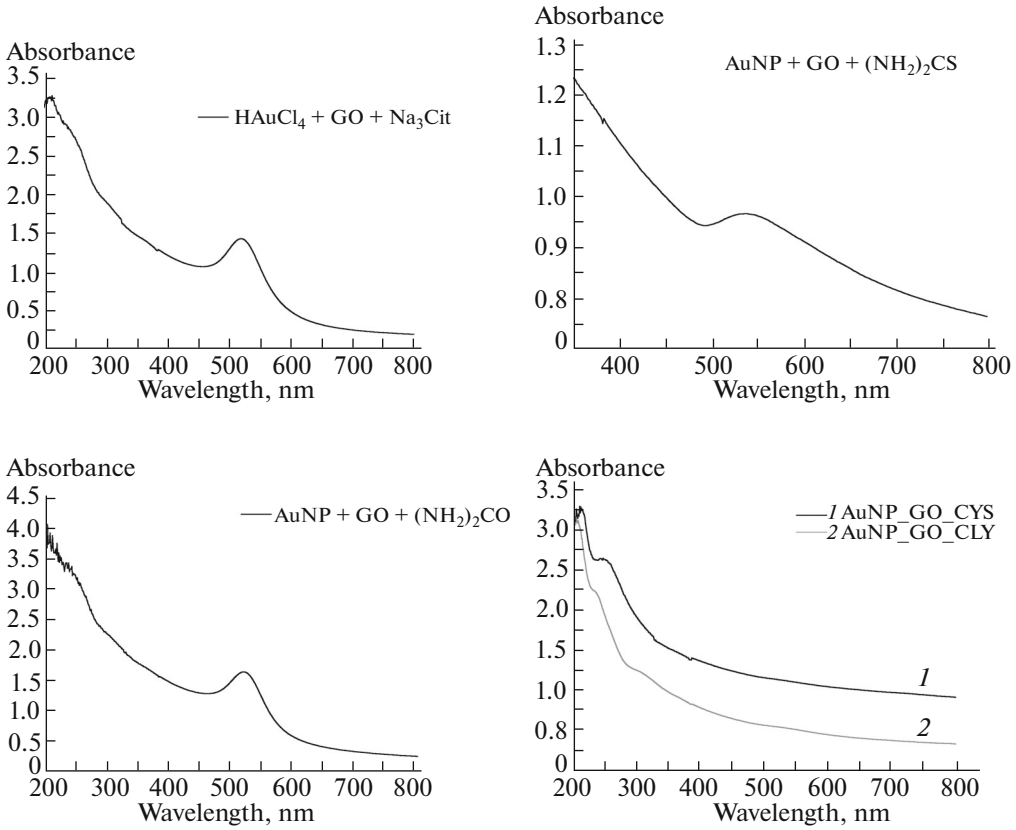

Fig. 6. Results of the UV–visible spectroscopy of the solutions of the gold nanoparticles obtained via the interaction of (a) aurichlorohydric acid, GO, and sodium citrate; (b) AuNP + RGO_$(NH_2)_2CS$; (c) AuNP + RGO_$(NH_2)_2CO$; and (d) AuNP + RGO_$(NH_2)_2CS$ and AuNP + RGO_$(NH_2)_2CO$.

the synthesized sample of GO (Fig. 7a). The gold nanoparticle–GO composite (Fig. 7b) retains the corrugated structure of GO on which the gold nanoparticles, the chemical nature of which is unambiguously confirmed by the data of the electron diffraction, are clearly visible. The mean size of gold nanoparticles determined from the statistical data processing is 15 ± 5 nm. The example of the microstructure of the composite consisting of the gold nanoparticles and RGO is presented in Fig. 7c. The chemical nature of the reducing agent affects the distribution of the gold nanoparticles over the surface of RGO. Thus, when urea is used as the reducing agent, the formation of the gold nanoparticles (16 ± 5 nm) distributed evenly over the surface of RGO is observed (Fig. 7c). During reduction with cysteine, the gold nanoparticles form agglomerates that cover the surface of RGO compactly. This is associated with the presence of two functional groups –SH and NH_2, which are capable of forming complexes with the gold ions, in cysteine. When glycine is used as the reducing agent, gold nanoparticles with a mean size of 12 ± 4 nm are mainly formed at the interlayer boundaries and defects of RGO.

Therefore, the data of TEM give evidence of the fact that the samples of GO reduced with cysteine and urea, which, as opposed to glycine, contains two functional groups participating in the formation of the bonds with the gold ions each, exhibit the greatest capacity for the conjugation with gold nanoparticles. These are $-NH_2$ and –SH in the case of cysteine and two $-NH_2$ in the case of urea.

Raman scattering spectroscopy is the method used most widely for an analysis of the material on the basis of GO. Two characteristic D and G bands in the regions of 1340 and 1590 cm^{-1}, respectively, are present in the RS spectra of the material on the basis of GO [8–12].

In Fig. 8, the RS spectrum of the sample of GO obtained using the laser with the wavelength of 633 nm is presented. The D band (the disorder-induced band) is associated with the formation of defects determined by the introduction of the heteroatoms of hydrogen and oxygen and the transition of part of carbon atoms in the sp^3-hybridization state (~1340 cm^{-1}) on the surface of graphite. The G band characterizes the oscillations of the system of the sp^2 carbon bonds (~1580 cm^{-1}) (the graphite-like region). The mean size of the ordered sections $L = 5600/E_e^4(I_D/I_G)^{-1}$ [A], where

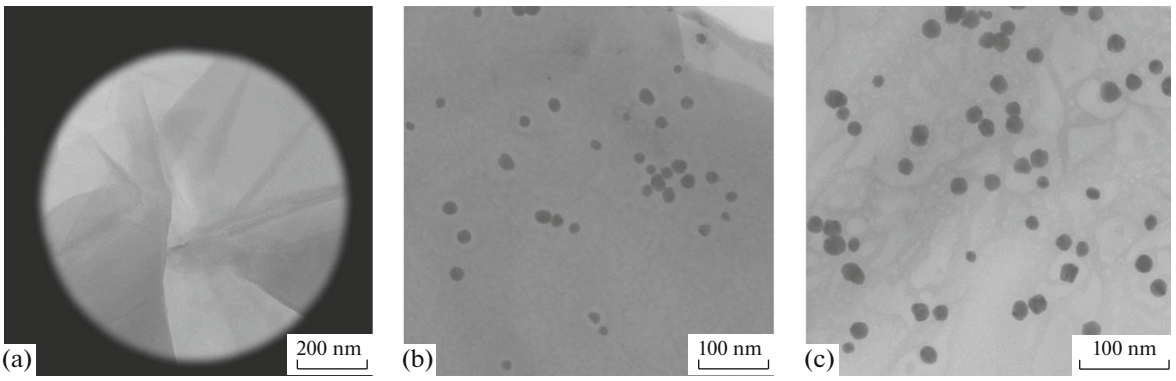

Fig. 7. Data of the TEM of (a) GO, (b) gold nanoparticles–GO composite, and (c) gold nanoparticles–GO reduced with urea composite.

E_e is the energy of the laser, can be determined from the ratio of the intensities I_D/I_G. The larger L is, the fewer defects there are [8]. In case of the laser used in this work, $E_e = 2.41$ eV.

In this work it is proposed to use the ratios of the intensities of the bands I_D/I_G, which is 1.03 for initial GO, as the disorder criterion. The results of the RS spectroscopy for the samples of RGO with various chemical prehistories are presented in Fig. 9 and Table 2.

It is obvious from the data presented in Table 2 that the mean size of the ordered sections of GO increases depending on the reducing agent as follows: cysteine < thiourea < glycine < urea.

The results of RS spectroscopy for the composites consisting of the gold nanoparticles and RGO are presented in Fig. 10 and Table 3.

It is obvious from the data presented in Table 3 that the gold nanoparticles promote the additional reduction of GO, which is accompanied by the decrease in the ratio of the intensities of the D and G bands. The mean size of the ordered sections of GO with the gold nanoparticles changes depending on the prehistory of the reducing agent in the same order as in the case of the materials free of gold, i.e., cysteine < thiourea < glycine < urea. Apparently, the reduction of GO with the nitrogen-containing reagent is the rate-determining step of the process of reduction of composite materials.

STUDY OF THE RS SPECTRA OF METHYLENE BLUE

In this work, the solution of methylene blue staining with the concentration of 10^{-6} M (Fig. 11, Table 4) was used as the model object for RS spectroscopy. The positions of all bands of the spectrum agree with the literature data.

It follows from the results of RS spectroscopy that the most substantial enhancement of the signal from

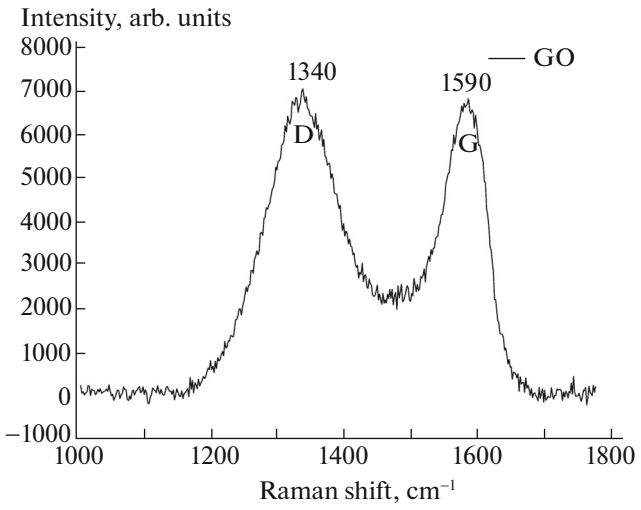

Fig. 8. RS spectrum of the sample of GO.

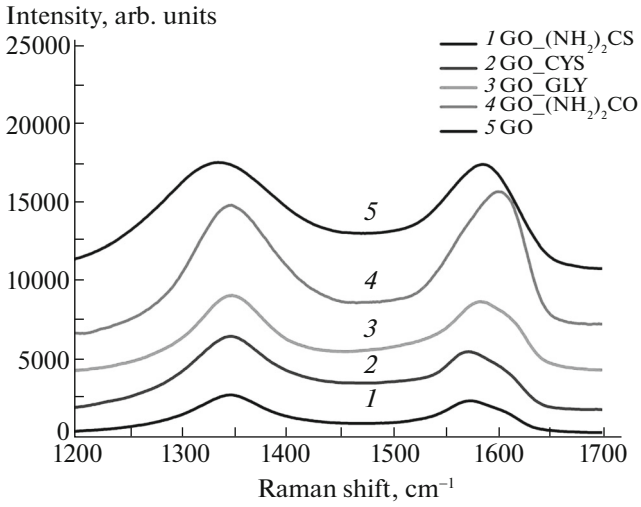

Fig. 9. RS spectra of the samples of RGO with various chemical prehistories.

Table 2. Analysis of the RS spectra of the samples of RGO with various chemical prehistories

Name of the sample	Reducing agent	Position of the D band, cm^{-1}	Position of the G band, cm^{-1}	I_D/I_G	L, Å
GO		1340	1590	1.03	160
RGO_$(NH_2)_2CS$	$(NH_2)_2CS$	1345.39	1578.76	1.52	100
RGO_CYS	Cysteine	1352.88	1575.13	1.67	99
RGO_GLY	Glycine	1352.88	1582.32	1.209	137
RGO_$(NH_2)_2CO$	$(NH_2)_2CO$	1349.88	1599.99	0.917	181

Table 3. Analysis of the RS spectra of the gold–RGO composites

Name of the sample	Reducing agent	Position of the D band, cm^{-1}	Position of the G band, cm^{-1}	I_D/I_G	L, Å
AuNP + GO		1332.38	1600.32	1.17	142
AuNP + RGO_$(NH_2)_2CS$	$(NH_2)_2CS$	1335.93	1603.73	1.241	134
AuNP + RGO_CYS	Cysteine	1330.61	1598.61	1.244	133
AuNP + RGO_GLY	Glycine	1331.75	1592.88	1.132	147
AuNP + RGO_$(NH_2)_2CO$	$(NH_2)_2CO$	1338.85	1596.3	0.897	185

methylene blue is observed in the case of the application of its solution onto the individual gold nanoparticles followed by the composite consisting of gold nanoparticles and GO reduced with urea and the least enhancement of the signal is observed in the case of the use of the composite consisting of the gold nanoparticles and unreduced GO. The data obtained in this work evidence the fact that the resonance absorption by gold nanoparticles in the region of the wavelengths close to the wavelength of the excitation laser and the increase in the mean size of the ordered sections of the samples on the basis of GO and gold nanoparticles are important factors for the enhancement of the signal in RS spectroscopy. The sample reduced with urea, for which the minimum ratio I_D/I_G is observed, possesses the largest sizes of the ordered sections in RGO and exhibits the most substantial enhancement of the signal from methylene blue when compared with other composites on the basis of RGO studied in this work.

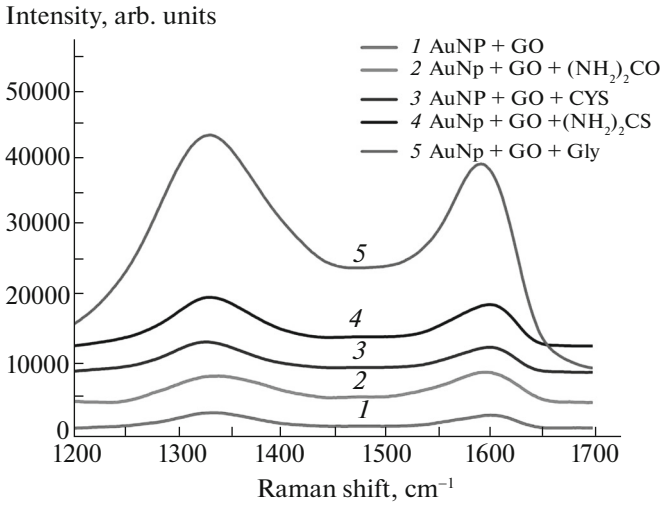

Fig. 10. RS spectra of the gold–RGO composites.

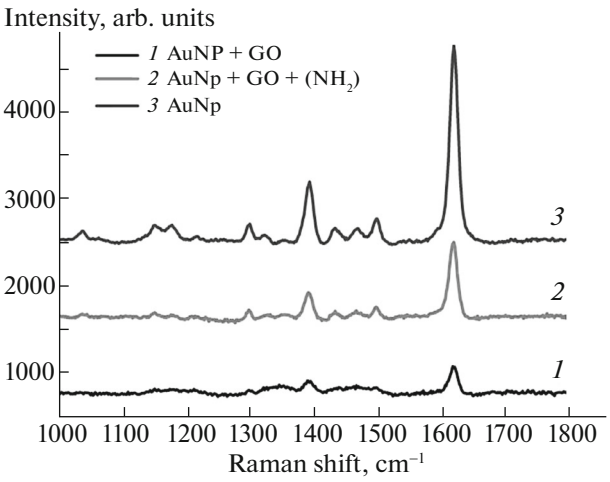

Fig. 11. RS spectra of the 10^{-6} M solution of methylene blue.

Table 4. Characteristic bands of methylene blue in the RS spectrum

Raman shift	Oscillations
1623	$\nu(C-C)_{ring}$
1396	$\nu(C-N)_{as}$
1303	$\nu(C-N)$
1153	$\beta(C-H)_{plane}$

CONCLUSIONS

Resonance absorption by gold nanoparticles in the region of wavelengths close to the wavelength of the excitation laser and the increase in the mean size of the ordered sections of the materials on the basis of RGO are important factors for the enhancement of the signal from the analyte molecules in RS spectroscopy. The derivatives of urea are the most effective reducing agents for GO. Apparently, the reduction with the derivatives of urea results in a decrease in the number of carboxylic groups and in an increase in the number of nitrogen-containing functional groups on the surface of the carbon-containing material, which enhances the effectiveness of the conjugation of the noble metal nanoparticles.

ACKNOWLEDGMENTS

This work was financially supported by the Russian Foundation for Basic Research (projects nos. 13-08-00657 and 13-03-01143).

REFERENCES

1. M. Moskovits, "Persistent misconceptions regarding SERS," Phys. Chem. Chem. Phys., No. 15, 5301–5311 (2013).
2. X. Ling, L. M. Xie, Y. Fang, H. Xu, H. L. Zhang, J. Kong, M. S. Dresselhaus, J. Zhang, and Z. F. Liu, "Can graphene be used as a substrate for Raman enhancement?," Nano Lett., No. 10, 553–561 (2010).
3. M. E. Kompan, F. M. Kompan, P. V. Gladkikh, E. I. Terukov, V. G. Rupyshev, and Yu. V. Chetaev, "Thermal conductivity of a composite medium with a disperse graphene filler," Tech. Phys. **56** (8), 1074 (2011).
4. Liang Zhou, Huaimin Gu, Can Wang, Juling Zhang, Meng Lv, and Ruoyu He, "Study on the synthesis and surface enhanced Raman spectroscopy of graphene-based nanocomposites decorated with noble metal nanoparticles," Colloids Surf. A: Physicochem. Eng. Aspects, No. **430**, 103–109 (2013).
5. W. S. Hummers and R. E. Offeman, "Preparation of graphitic oxide," J. Am. Chem. Soc. **80** (6), 1339–1339 (1958).
6. J. Turkevich, P. C. Stevenson, and J. Hillier, "The formation of colloidal gold," J. Phys. Chem., No. 57, 670–673 (1953).
7. J. A. Peck, C. D. Tait, B. I. Swanson, and G. E. Brown, "Speciation of aqueous gold(III) chlorides from ultraviolet/visible absorption and Raman/resonance Raman spectroscopies," Geochim. Cosmochim. Acta **55**, 671–676 (1991).
8. F. Tuinstra and J. L. Koenig, "Raman spectrum in graphite," J. Chem. Phys. **53**, 1126–1130 (1970).
9. D. R. Dreyer, P. Sungjin, C. W. Bielawski, and R. S. Ruoff, "The chemistry of graphene oxide," Chem. Soc. Rev., No. 39, 228–240 (2010).
10. Shengtong Sun and Peiyi Wu, "Competitive surface-enhanced Raman scattering effects in noble metal nanoparticle-decorated graphene sheets," Phys. Chem. Chem. Phys. **13**, 21116–21120 (2011).
11. A. N. Sidorov, G. W. Sławin'ski, A. H. Jayatissa, F. P. Zamborini, and G. U. Sumanasekera, "A surface-enhanced Raman spectroscopy study of thin graphene sheets functionalized with gold and silver nanostructures by seed-mediated growth," Carbon, No. **50**, 699–705 (2012).
12. Xing Ma, Qiuyu Qu,Yun Zhao, Zhong Luo, Yang Zhao, Kee Woei Ng, and anli Zhao, "Graphene oxide wrapped gold nanoparticles for intracellular Raman imaging and drug delivery," J. Mater. Chem. B, No. 1, 6495–6500 (2013).

Translated by E. Boltukhina